THE NORTH ATLANTIC CURRENT SYSTEM:

A SCIENTIFIC REPORT

19-20 April 1993

Woods Hole Oceanographic Institution

Woods Hole, MA 02543

Edited by:

Paola Malanotte-Rizzoli
Massachusetts Institute of Technology
Cambridge, MA 02139

Thomas Rossby
University of Rhode Island
Narragansett, RI 02882

Modeling the Subpolar North Atlantic

C.W. Böning, F.O. Bryan, and W.R. Holland
National Center for Atmospheric Research
P.O. Box 3000
Boulder, CO 80307

In contrast to the tropical and midlatitude Atlantic, or for the Arctic, there is not a long history of modeling of the subpolar region of the North Atlantic. Model simulations of the thermohaline circulation with grid resolutions that capture the small-scale frontal structures and eddies of the high latitudes have become possible only very recently. The discussion of problems and achievements in the simulation of the North Atlantic Current (NAC) system presented here will be based mainly on results from the "Community Modeling Effort" (CME). Following the initial model run of Bryan and Holland (1989), a series of experiments have been conducted by the groups at NCAR and in Kiel that explore the sensitivity to a variety of factors such as atmospheric forcing, model resolution, and lateral boundary conditions.

Previous evaluations of the model results and detailed comparisons with observations were focused mainly on the tropical and subtropical North Atlantic. The present, preliminary analysis of the model behavior in the subpolar North Atlantic indicates horizontal resolution and thermohaline forcing to be of critical importance to the mean circulation. Compared to the subtropics and tropics, the solution is much less sensitive to the wind stress climatology. We shall discuss the influence of these model factors following a brief outline of the model configuration, and a general overview of the model circulation in the subpolar North Atlantic.

1. Model configuration

The model of the wind- and thermohaline-driven circulation in the Atlantic Ocean is based on the Geophysical Fluid Dynamics Laboratory (GFDL) primitive equation model. The model domain extends from 15°S to 65°N (Fig. 1). There are 30 vertical levels, their spacing smoothly increasing from 35 m at the surface, to 100 m near 500 m depth, and 250 m below 100 m depth. The thermohaline circulation is driven by a relaxation of surface salinity to the monthly mean values of Levitus (1982) on a time scale of 50 days, and a linear bulk formula for the surface heat flux, i.e., a relaxation to observed "effective" air temperatures.

In what we will refer to as the "standard" configuration of the model, the northern and southern (wet) boundaries are closed to normal flow. In the last five grid cells adjacent to these boundaries, potential temperature (T) and salinity (S) are restored to the monthly mean values of the Levitus' (1982) climatology. The rationale for the buffer zones is to include the effect of water mass transformations taking place outside of the model domain. At present there is no ice model included. To prevent the occurrence of super-cooled water due to the strong winter heat losses, the water temperatures over the northern portion of the Labrador Shelf are restored to climatology.

A suite of model experiments has been carried out to explore the effect of different model factors and parameterizations and the sensitivity to various aspects of the atmospheric forcing. There are three basic versions: with a horizontal resolution (meridional x zonal) of 1° x 1.2°, 1/3° x 0.4°, and 1/6° x 0.2°. We will refer to these as the medium-resolution (MR), high-resolution (HR), and very-high resolution (VR) versions. For the HR and VR models, a biharmonic scheme is used for horizontal diffusion and viscosity, whereas an isopycnal diffusion scheme is adopted for the MR model to account for the mixing effect of mesoscale eddies.

2. Model features in the subpolar North Atlantic

The most prominent feature of the upper-layer flow field in the HR and VR cases is the band of energetic eddy activity straddling the course of the NAC (Fig. 2). The distribution of eddy variability is similar for the HR and VR cases, but the energy is about twice as high in the VR case. The maximum energies in that case are close to the observed values of about 1000 cm^2s^{-2} in the Newfoundland Basin east of Flemish Cap, as given by drifting buoy or Geosat altimeter data (Beckmann et al., 1993). Apart from its influence on the quantitative representation of the instability processes, the different resolution of the MR and VR cases has only a minor impact on the mean circulation in the subpolar ocean. The discussion of the mean flow properties will, therefore, be based on the HR (and, in the subsequent section, MR) case.

Mean upper-layer fields are depicted in Fig. 3 for the HR case in "standard" configuration, that is with a closed boundary at 65°N and restoring to Levitus' T and S in a 1.67°-wide buffer zone. Despite the long-term averaging, the subarctic front in the northwest corner region is remarkably sharp, indicative of only little meandering in that area, and little cross-frontal exchange of the warm, salty waters in the Newfoundland Basin with the cold, fresh water of the Labrador Sea. (The eddy activity has its maximum in the Newfoundland Basin, and there is a sharp drop of eddy energy across the front in the NW corner.) An outstanding, unrealistic feature of the solution concerns the northward flowing current along the Grand Banks: it is pressed against the continental slope, with the bulk of the water carried through Flemish Pass. Possibly related to that, the Labrador Current is blocked at the northern edge of the Grand Banks and a wedge of cold, fresh Labrador Shelf water is drawn eastward along the subarctic front. The cause of these local model problems is, as yet, unknown.

Another major unrealistic feature of the mean fields depicted in Fig. 3 is the downstream course of the NAC. Instead of extending northeastward into the Icelandic Basin, the flow turns northward already at about 35°W, leaving the northeastern basin too cold and far too quiet energetically. As will be discussed below (section 4), that behavior is related to the conditions applied at the northern wall. About one half of the 22 Sv carried northward by the NAC recirculates horizontally with the cyclonic gyre of the subpolar North Atlantic, the other half is transformed to deep water and carried southward with the DWBC in the Labrador Sea (Figs. 4 and 5). However, there is no continuation of the DWBC along the Grand Banks. At about 50°N (just north of the axis of the NAC), the DWBC separates from the continental slope and is deflected eastward, eventually turning southward again near the mid-Atlantic Ridge. A similar behavior has been observed in model experiments with coarser resolution (Gerdes, 1988) and may be seen also in the 1/2° World Ocean model of Semtner and Chervin (1992). It remains to be seen whether this apparently robust model behavior is related to the local problems of the upper-layer flow in the Grand Banks area.

3. Influence of horizontal resolution

While differences in the mean flow patterns of HR and VR cases are minor, there is an important difference between the non-eddy resolving (MR) and the eddy-resolving cases, concerning the location of the subarctic front (Fig. 6). In the high resolution cases, the front is not only sharpened, it is also shifted to the north by about 5° of latitude. Consequently, surface temperatures over a large area of the Newfoundland Basin are significantly higher than in the MR case. The shift of the front, roughly to its observed location, has a profound impact on the surface heat budget, partially remedying a typical problem of low resolution models (Fig. 7). As a consequence of their much too cold surface temperatures in the Newfoundland Basin, non-eddy resolving models like the present MR version, or the models of Sarmiento (1986) and Gerdes (1988), all show a strong heat uptake of the ocean in that area, locally exceeding 100 wm^{-2}. The dynamical mechanism of the drastically different behavior of the eddy-resolving cases has yet to be studied; this feature demonstrates, however, the importance of model resolution for an adequate representation of the mean flow properties in this area.

4. Effect of the northern boundary condition

To avoid the explicit numerical representation of the overflow processes across the Greenland-Scotland-Ridge system, a closing of the North Atlantic near the ridge has been a common practice in various models, e.g., Sarmiento (1986) and Semtner and Chervin (1992). The effect of the water mass transformations taking place north of Iceland are taken into account by buffer zones in which T and S are restored to observed values. Two problems associated with the standard use of climatological values for T and S as given by Levitus (1982) are noted here:

In spatially smoothed climatological data, the signature of Denmark Strait Overflow Water (DSOW), which is tightly pressed against the continental slope of Greenland, is almost completely lost; i.e., in the Levitus' data there is no water with temperatures less than 3°C south of the Denmark Strait. The lack of the cold (~0°C) DSOW-core in the buffer zone has important consequences for the thermohaline circulation (Fig. 8): southward transport is mostly confined to the upper NADW-range, above ~2500 m and >3°C. Using restoring temperatures based on actual section data that include the signature of DSOW south of the Denmark Strait has a damatic impact on the deep flow field and the meridional overturning (Döscher et al., 1993).

The narrowness of the buffer zone and the positioning of the northern boundary may have a deleterious effect on the upper-layer flow, i.e., the path of the NAC. Because the buffer zone does not extend south of Iceland, in order to satisfy mass conservation, the upper-layer water to be converted to DSOW must be drawn into the buffer zone between Greenland and Iceland, rather than to the east of Iceland. Thus, the buffer zone formulation, meant to help in the simulation of the large-scale thermohaline circulation, is incompatible with a large fraction of the NAC flowing into the Northeast Atlantic. Open boundary conditions may be a solution to this problem, and work is underway to test different formulations.

References

Beckmann, A., C.W. Böning, B. Brügge, and D. Stammer, 1993: Eddy variability in the central North Atlantic Ocean: Results from satellite altimetry, surface drifters, and numerical modeling, submitted to J. Phys. Oceanogr.

Bryan, F.O., and W.R. Holland, 1989: A high resolution simulation of the wind- and thermohaline-driven circulation in the North Atlantic Ocean, Special Report, University of Hawaii, 99-115.

Döscher, R., C.W. Böning, and P. Herrmann, 1993: Response of meridional overturning and heat transport in the North Atlantic to changes in thermohaline forcing in northern latitudes: A model study, submitted to J. Phys. Oceanogr.

Gerdes, R., 1988: Die Rolle der Dichtediffusion in numerischen Modellen der Nordatlantischen Zirkulation. Ber. Inst. f. Meereskunde, Kiel, No. 179, 176 pp.

Isemer, H.-J., and L. Hasse, 1987: The BUNKER Climate Atlas of the North Atlantic Ocean, Vol. 2: Air-Sea Interactions, Springer-Verlag, Berlin, 256 pp.

Levitus, S., 1982: Climatological Atlas of the World Ocean, NOAA Prof. Paper 13, U.S. Government Printing Office, 173 pp.

Sarmiento, J.L., 1986: On the North and Tropical Atlantic heat balance, J. Geophys. Res., 91, 11677-11698.

Semtner, A.J. and R.G. Chervin, 1992: Ocean general circulation from a global eddy-resolving model, J. Geophys. Res., 97, 5493-5550.

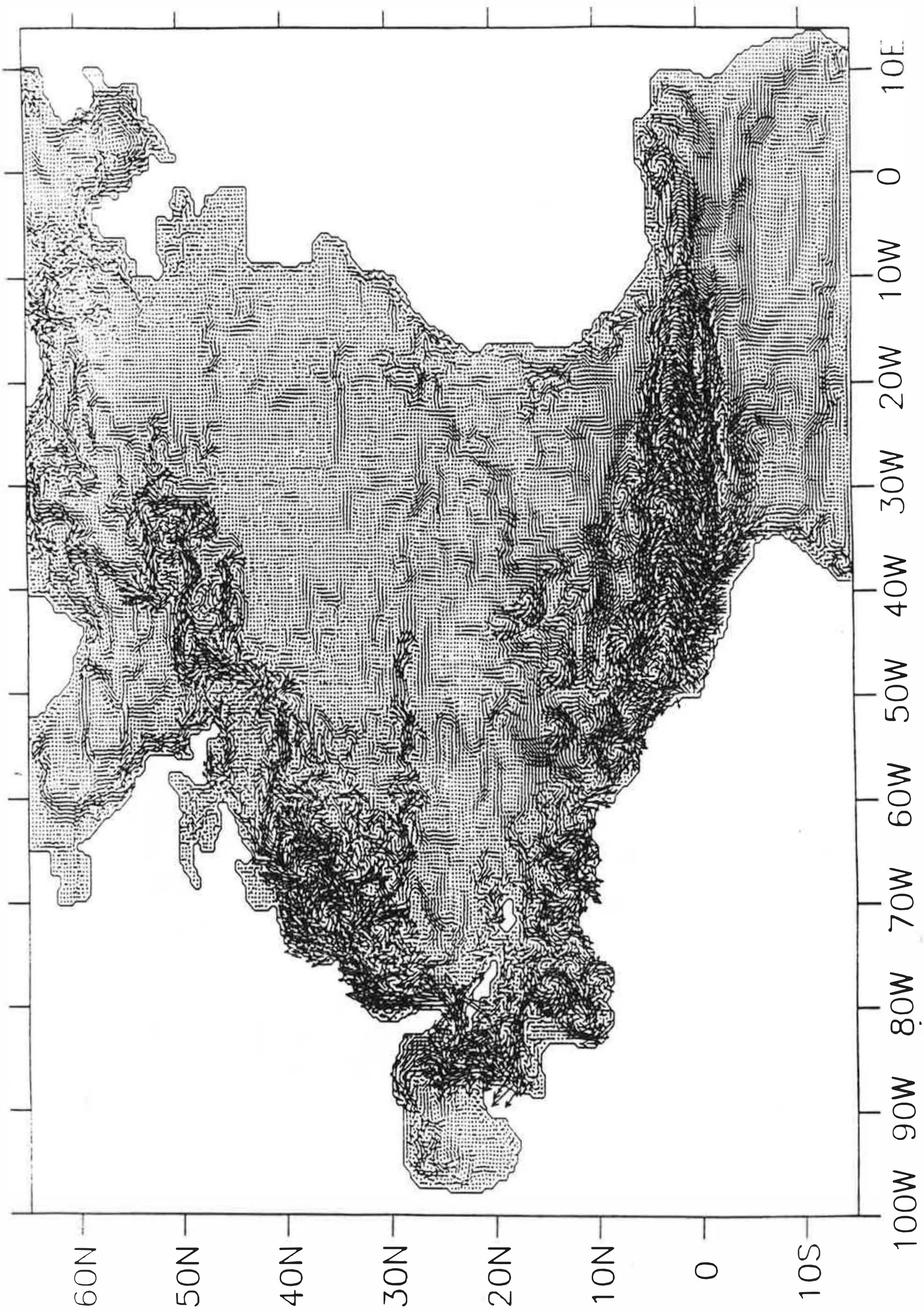

Fig. 1 Instantaneous flow field at a near-surface level (91 m), for the high-resolution version (1/3° × 0.4°) of the CME.

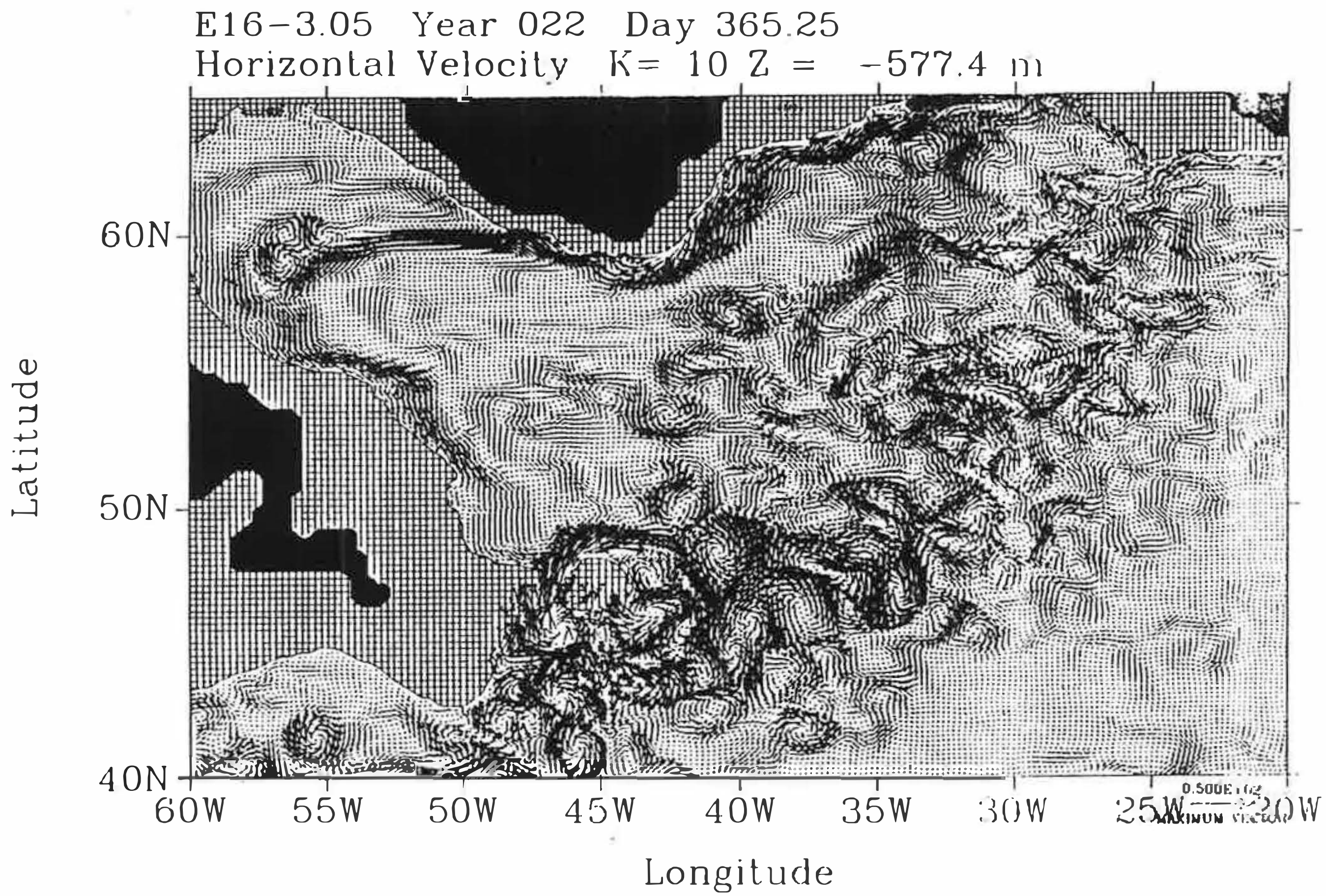

Fig. 2 Instantaneous flow field at 577 m depth in the subpolar North Atlantic, for the very-high resolution version (1/6° × 0.2°).

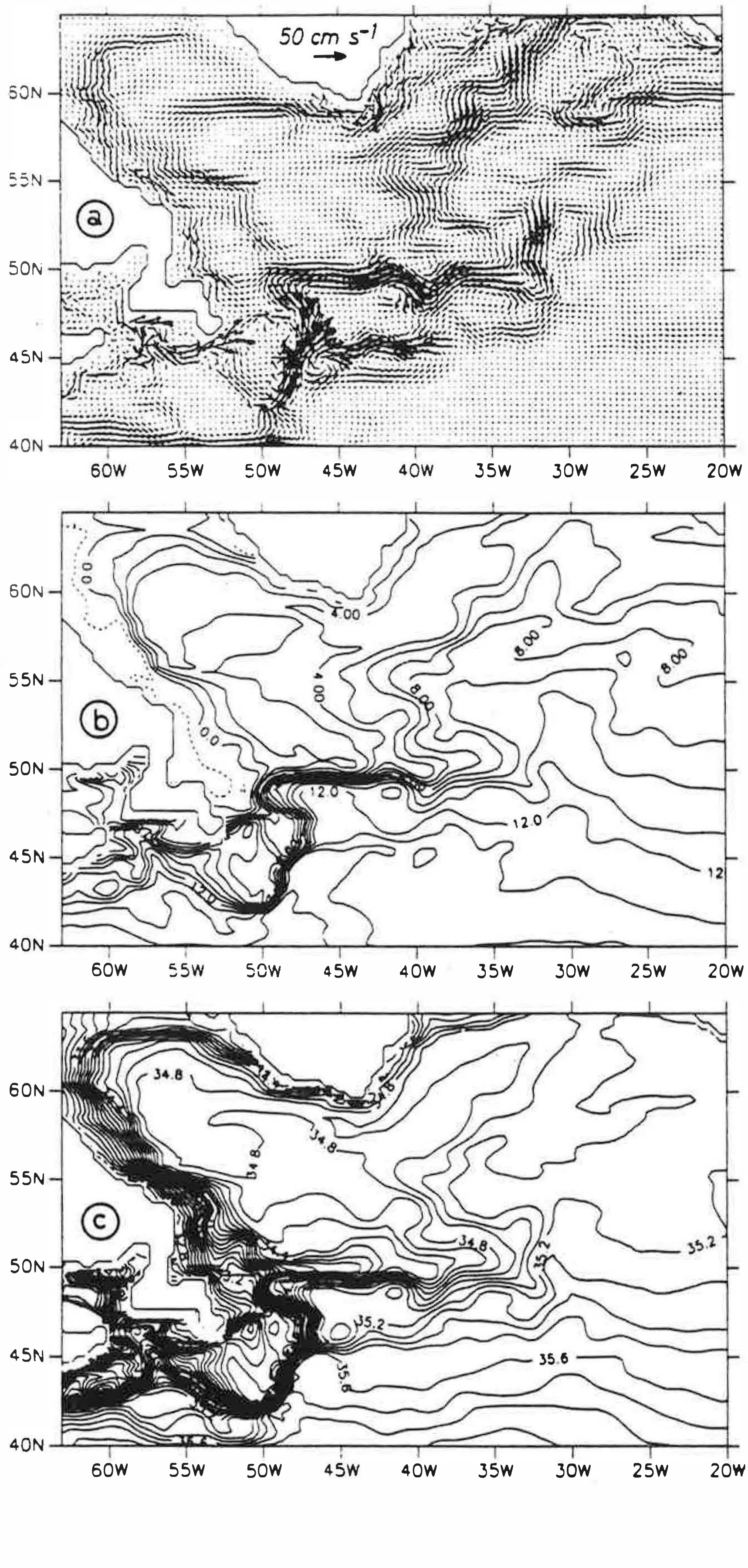

Fig. 3 Mean fields (5-year averaging) of surface velocity, potential temperature, and salinity in the subpolar North Atlantic, for the high-resolution version (1/3° × 0.4°).

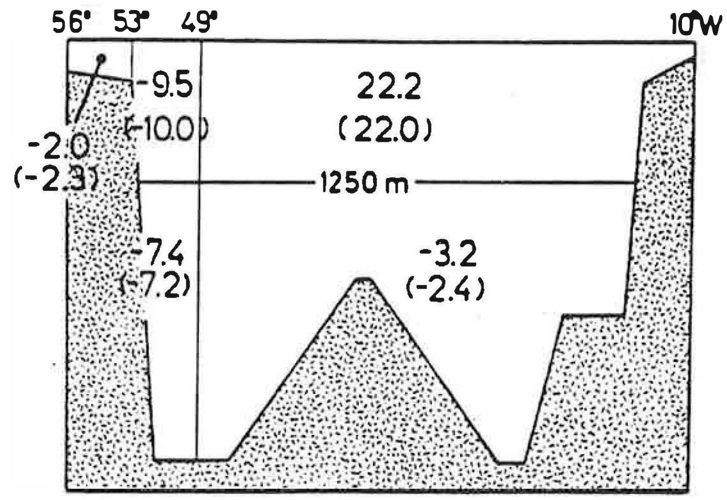

Fig. 4 Meridional volume transports (in Sv) through a cross-section along 53.5° N; HR-version with Levitus' buffer zone and forcing with Hellerman-Rosenstein wind stresses; in parenthesis: forcing with Isemer-Hasse wind stresses.

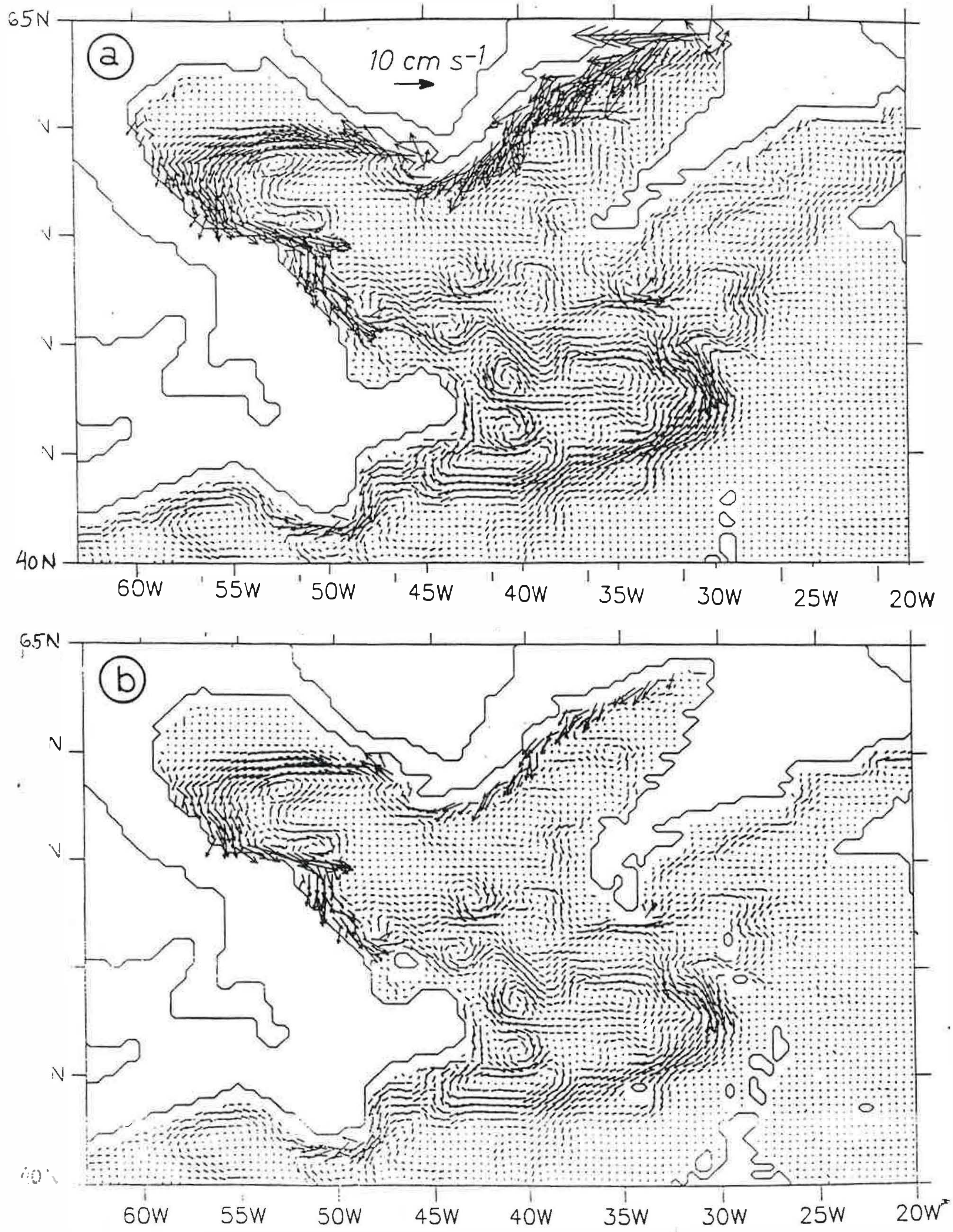

Fig. 5 Mean flow fields at 1875 m (a) and 2375 m (b) depths; high-resolution case with Levitus' buffer zone.

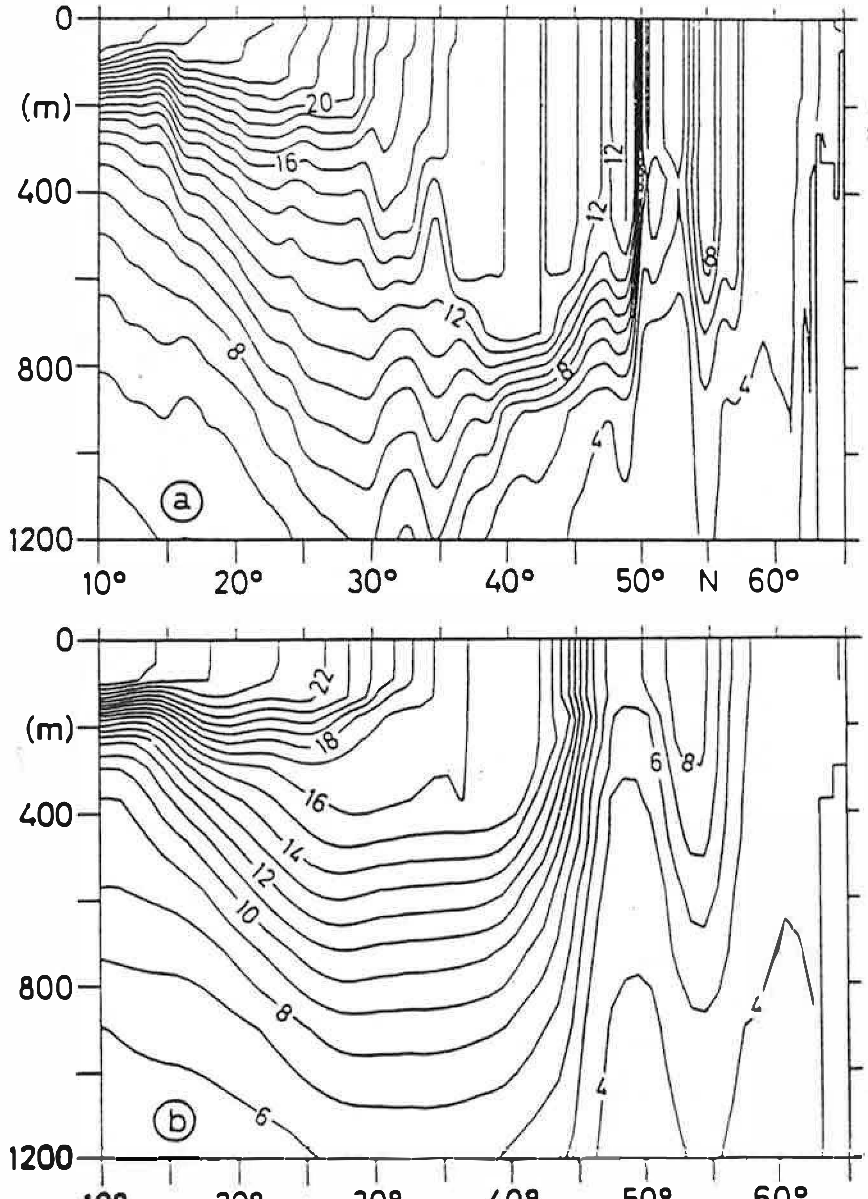

Fig. 6 Meridional sections of potential temperature in late winter (day 90) along 40° W, for a high-resolution case (a), and a medium-resolution case (b), with identical forcing.

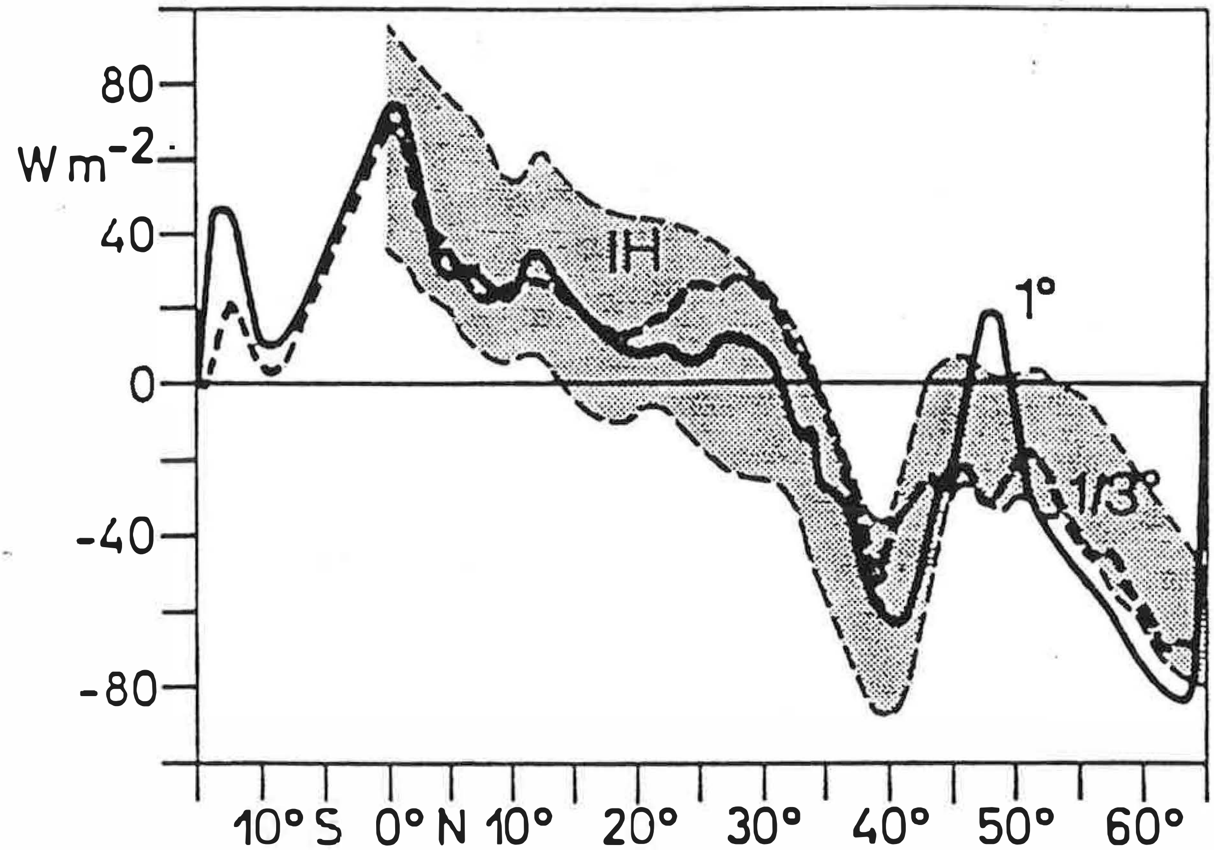

Fig. 7 Surface heat flux, zonally-averaged across the Atlantic Ocean, for the two model cases of Fig. 6; the shaded area indicates the range of uncertainty of the observed heat flux, according to Isemer and Hasse (1987).

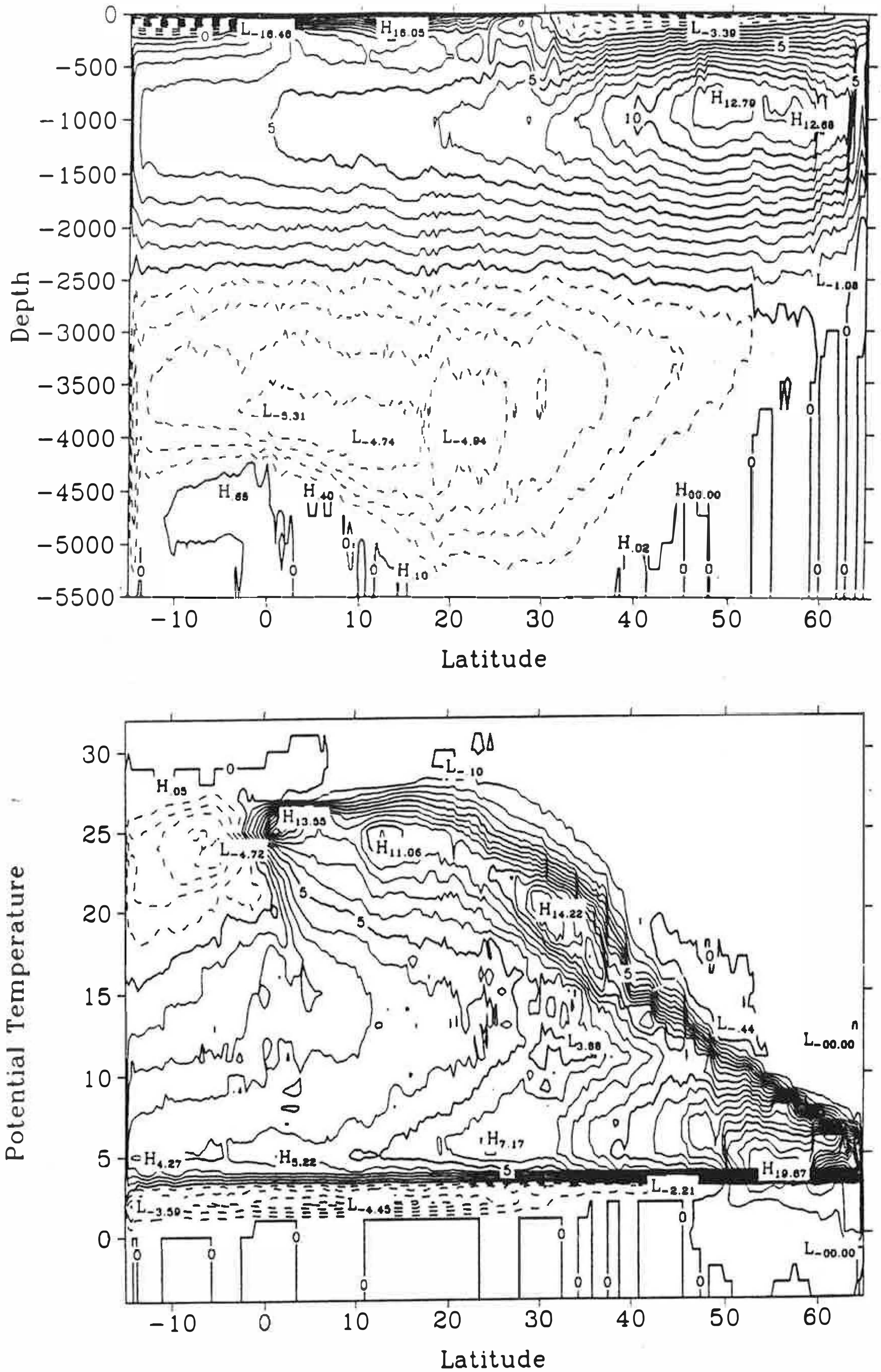

Fig. 8 Streamfunction (in Sv) of the zonally-averaged flow in (a) the latitude-depth plane, (b) latitude-potential temperature plane; for the high-resolution case in "standard" configuration (buffer zones with relaxation to Levitus' T and S).